2026 IEEE International Conference on Robotics and Automation (ICRA 2026)
June 1-5, 2026. Vienna, Austria

Perching-Based Haptic Guidance for Physical Human-Robot Interaction with Aerial Robots

Ayano Miyamichi[1] and Kei Okada[1]

***Abstract*— In recent years, the field of Human-Drone Interaction (HDI) has attracted significant attention, particularly in navigation assistance using aerial robots. However, existing approaches rely on non-contact cues or indirect physical connections such as cables, which demand continuous flight and high energy consumption. These limitations shorten interaction time and make direct assistance challenging. To address this issue, we employ a deformable aerial robot with inflatable structures that enables adaptive perching on the human arm. On this platform, we propose a perching-based haptic guidance method in which the robot maintains close contact to deliver directional cues via thrust modulation and provide alerts and arrival feedback through vibration signals. The system further switches haptics modes dynamically according to context, enabling intuitive and flexible guidance beyond conventional methods limited to simple directional cues. Through experiments, we quantitatively evaluated the presented force characteristics and confirmed that perching-based haptic guidance requires less power than continuous flight in the same platform. User experiments further demonstrated that participants could reach target locations without major deviations even when vision and hearing were blocked. Moreover, the entire process of approach, perching, haptic guidance, and deperching was stably executed on the real platform, validating the feasibility of perching-based haptic guidance. To the best of our knowledge, this is the first study to realize close physical Human-Drone Interaction (pHDI) through perching-based haptic guidance.**

I. Introduction

Recent advances in Human-Robot Interaction (HRI) have highlighted the growing importance of robotic assistance across domains ranging from disaster response to daily life [1], [2]. Aerial robots, in particular, offer high mobility, enabling access to environments difficult for ground robots to reach, such as crowded or cluttered spaces. This capability has led to the emergence of Human-Drone Interaction (HDI) as a distinct research field [3]–[5]. However, a fundamental challenge across all HDI applications is that continuous flight requires high energy consumption, which severely limits the duration of interaction [5]. This limitation also affects the field of aerial-robot-based guidance, where most existing studies have explored non-contact cues such as sounds or flight movements [6]–[8], as well as indirect contact through cables or tethers [9], [10]. In addition to the energy and time constraints inherent to flight, these guidance approaches also face challenges such as dependence on visibility, environmental conditions, and tether constraints, and they do not incorporate explicit signaling mechanisms to indicate task completion or arrival. Thus, most existing HDI guidance systems interact with users only during flight and have not yet achieved physical Human-Robot Interaction (pHRI), which requires close contact and direct assistance.

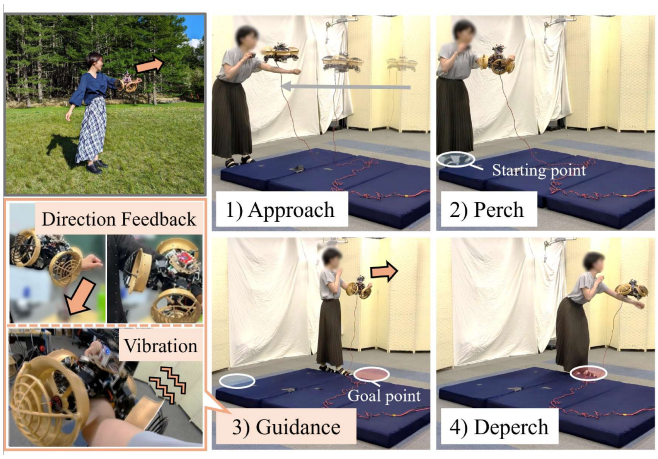

Fig. 1. Perching-based haptic directional guidance by aerial robot.

To address this challenge, we introduce perching as a new HDI interface that allows the aerial robot to temporarily stop flying, land, and grasp onto the user. While perched, it provides force-based haptic guidance through thrust distribution while maintaining close contact as shown in Fig. 1. In addition to directional guidance, the robot can also generate vibration cues to signal task completion or draw the user's attention. This enables the robot to provide intuitive and easy-to-understand haptic directional cues while maintaining stability and energy efficiency without sustained flight.

This framework enables share haptic information through direct physical contact, which has been difficult to achieve with conventional aerial robots, thereby opening up a wide range of applications. For example, in a fire emergency with poor visibility, an aerial robot could enter a building ahead of firefighters, perch on stranded evacuees, and guide them to an exit through haptic cues. In mountain rescue scenarios, it could perch on a survivor and physically guide them toward a safer or more visible location over an extended period, while conserving energy. In everyday use, the robot could perch on the arm or shoulder to guide walking, providing intuitive support for visually impaired users and the general public, even in noisy or crowded environments. These cases illustrate that perching-based haptic guidance not only reduces energy consumption but also extends the role of aerial robots into domains requiring sustained close pHRI.

[1] The authors are with the Department of Interdisciplinary Information Studies, Graduate School of Interdisciplinary Information Studies, The University of Tokyo, 7-3-1 Hongo, Bunkyo-ku, Tokyo, 113-8656, Japan. miyamichi@jsk.imi.i.u-tokyo.ac.jp

A. Related Work

1) Perching Aerial Robots: Aerial robots, with their high mobility, have been widely used in environments that are difficult for humans to access [11], [12], including surveillance [13], inspection [14], and disaster response [15]. However, continuous flight requires substantial energy, which limits their ability to perform long-duration missions or maintain stationary observations. To overcome this limitation, inspired by bird behavior, researchers have explored perching that allows aerial robots to land and grasp objects. Perching enables them to halt flight to conserve energy while acquiring high-quality data from a stable stationary state [16].

Existing perching aerial robots can be broadly divided into two categories. Some employ independent perching mechanisms, which separate flight and grasping but increase weight and size [17]–[28]. Others use deformable rotor-embedded arms, which are more compact but struggle to balance flight rigidity and grasping compliance [29]–[32]. Despite these differences, most perching aerial robots have been developed mainly for environmental monitoring and remain limited to rigid structures, without considering safe interaction with humans.

In contrast, recent work has introduced deformable aerial robots that integrate unilateral flexible rotor-embedded arms with pneumatic inflatable actuators [33]. The inflatable actuators provide compliance for safe grasping of soft targets such as the human arm, while the arm structure ensures the rigidity required for stable flight. These two functions were previously difficult to achieve simultaneously. In addition, the deformable arm design maintains a compact form that allows the robot to perch directly on a moving human arm without interfering with natural motion.

2) Navigation assistance in HDI: In recent years, research on HDI has rapidly advanced with the goal of enabling aerial robots to collaborate with humans in everyday environments [5]. HDI studies have explored a wide variety of applications, including communication through encoding human or robot motion and emotions [34]–[38], enhancement of physical activity and sports experiences [39]–[41], as well as health monitoring and triage [42]–[44]. Among these, navigation tasks that support human mobility have emerged as a key application, as aerial robots can provide guidance without requiring handheld or wearable devices, thereby reducing user burden and effectively leveraging their high mobility. Two main approaches to aerial robot navigation assistancehave been investigated, non-contact methods and haptic methods relying on indirect physical connections. Non-contact methods include approaches utilizing non-visual channels such as propeller sounds or airflow [6], [7], and methods expressing basic actions like straight flight or turning using the aerial robot's motion [8]. In contrast, haptic approaches with indirect physical connection include the work of Tognon et al. [9], who proposed connecting humans and aerial robots with a cable and guiding the user through tensile forces. Their study analyzed passivity and stability and confirmed effectiveness through user experiments. Similarly, GuideCopter [10] connected an aerial robot to a user's finger with a tether and pulled it to provide haptic cues for locating the hand position of visually impaired users, achieving more precise and intuitive guidance than voice-based systems.

Despite these promising results, existing methods still face challenges. Non-contact approaches depend on visibility and environmental conditions, while tether-based methods require physical constraints. Furthermore, across most HDI studies, the high energy consumption of continuous flight has been highlighted as a critical limitation that shortens interaction time [5]. Thus, most existing HDI systems are confined to flight-based interaction relying on either non-contact cues or indirect physical connections, leaving close pHRI and direct assistance largely unexplored.

In contrast, birds in nature, such as trained falcons or pet birds, can physically contact humans by perching on shoulders or arms not only for rest but also as a means of bonding and communication [45], [46]. Inspired by this behavior, we propose a new approach in which an aerial robot perches directly on a human arm and provides haptic guidance through thrust modulation, delivering both vibration signals and directional feedback while the robot remains in close physical contact. This approach achieves stable and energy-efficient interaction without sustained flight and opens a new pathway for intuitive and more intimate physical Human-Drone Interaction (pHDI).

B. Contributions

The contributions of this study are threefold:

- **Realization of pHDI by perching-based guidance**
  We introduce a new framework for physical Human-Drone Interaction (pHDI) by enabling an aerial robot to perch directly on the human arm and maintain close physical contact for haptic guidance.
- **Design of haptics guidance control method**
  We design a thrust distribution method to present clear directional forces, and we introduce context-dependent mode switching between pulsed directional cues and vibration alerts.
- **Integrated implementation and validation**
  We validate the system, demonstrating that it successfully performs the full sequence of perching, haptic guidance, and deperching to guide participants to target positions.

To the best of our knowledge, this is the first approach that enables an aerial robot to provide haptic guidance while maintaining close physical contact with a human, thereby realizing the closest and unconstrained pHDI.

C. Paper Organization

The remainder of this paper is organized as follows. Section II describes the proposed perching-based haptic guidance method, including thrust-based directional cue generation and context-adaptive mode switching. Section III presents the experimental results, including user studies on guidance performance. Finally, Section IV summarizes the findings and discusses future work.

II. Method

A. Configuration of a Deformable Aerial Robot for Perching on a Human Arm

In this study, the aerial robot which is designed to perch safely on a human arm as illustrated in Fig. 2, is employed as the platform to validate the effectiveness of the proposed haptic guidance method. It is a deformable aerial robot that integrates unilateral flexible rotor-embedded arms with pneumatic inflatable actuators. The unilateral flexible arm is designed so that each link braces against the others through upward thrust, enabling the structure to rigidify during flight and ensure stable attitude control. At the same time, pneumatic inflatable actuators are embedded in each joint and at the contact surfaces. During perching, they absorb landing impacts and allow the arm to conform to the shape of the target, enhancing adaptability. This design enables the robot to safely grasp soft targets such as a human arm without causing discomfort, while maintaining a stable hold even if the user moves or shakes their arm. By combining these two mechanisms, the system achieves both rigidity during flight and adjustable compliance during grasping, a combination that has been difficult to realize in previous designs.

The pneumatic control system is also designed for efficiency. In addition to pressurization from the pump, it leverages airflow from the contact parts to the joints to accelerate arm deformation during perching. After grasping, the flow channel design enables energy-efficient holding without the need for additional pressurization as long as the actuators remain intact. Furthermore, the target pressures are determined based on grasping experiments with a human-arm model, setting each section to the pressure value that produced the maximum grasping force. These design considerations ensure that the robot can securely perch on a human arm while minimizing energy consumption.

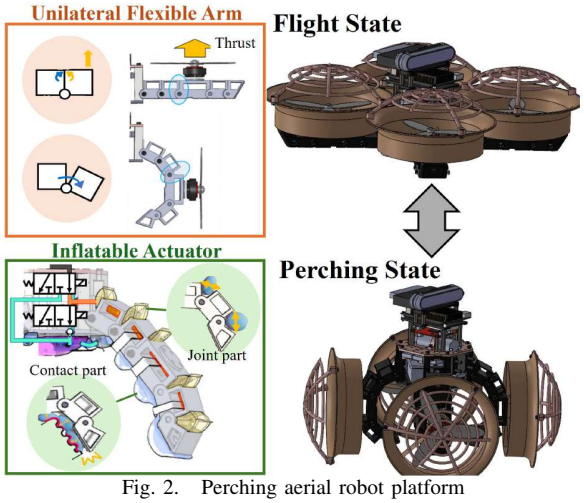

Fig. 2. Perching aerial robot platform

B. Thrust-Based Haptic Direction Generation

The aerial robot in this study provides haptic guidance for intuitive navigation assistance by estimating the desired direction from the target position and the robot's attitude, and then distributing thrust moments to the motors accordingly. The conceptual model used to compute the haptic guidance direction and thrust allocation is illustrated in Fig. 3. The difference vector between the robot's current position $\mathbf{p}_{current}$ and an arbitrarily defined target position $\mathbf{p}_{target}$ is used as the reference for haptic direction. Its normalized form is defined as the presented force direction:

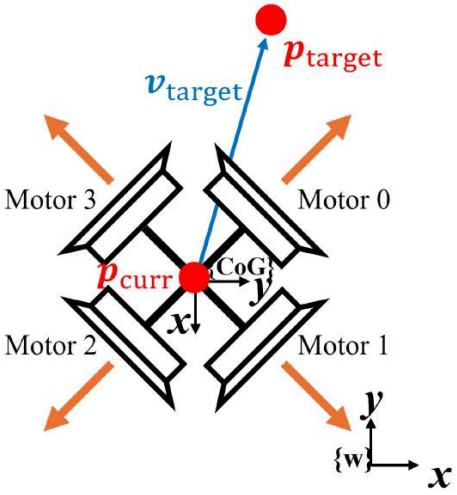

Fig. 3. Calculation model of haptic guidance direction

$$\mathbf{v}_{target} = \mathbf{p}_{target} - \mathbf{p}_{current} \tag{1}$$

$$\mathbf{f} = \frac{\mathbf{v}_{target}}{\|\mathbf{v}_{target}\|} \tag{2}$$

Subsequently, as a premise of the thrust allocation design, this study assumes that during perching each motor generates thrust only in the horizontal direction, while the vertical component can be neglected. The four motors are assumed to be evenly arranged at 90° intervals along diagonal directions (±45° and ±135°) in the xy-plane of the body coordinate system, each capable of generating equal thrust. Under these assumptions, the matrix of base direction vectors of the motors $\mathbf{M}_{base}$ are defined as:

$$\mathbf{M}_{base} = \begin{bmatrix} -1 & -1 & 1 & -1 \\ 1 & 1 & -1 & -1 \end{bmatrix} \tag{3}$$

Using the rotation matrix $\mathbf{R}$ representing the robot's attitude, the actual thrust direction vectors of the motors are then computed as:

$$\mathbf{M} = \mathbf{R}\mathbf{M}_{base} \tag{4}$$

The thrust coefficients of the motors are denoted as $\boldsymbol{\alpha} = [\alpha_1, \alpha_2, \alpha_3, \alpha_4]^\top$, and are treated as unknown variables to be optimized. To ensure that the synthesized thrust vector $\mathbf{M}\boldsymbol{\alpha}$ matches the desired direction vector $\mathbf{f}$, the following least-squares problem is formulated:

$$\min_{\boldsymbol{\alpha} \geq 0} \|\mathbf{M}\boldsymbol{\alpha} - \mathbf{f}\|_2^2 \tag{5}$$

The thrust coefficients $\boldsymbol{\alpha}$ are subject to non-negativity constraints and are iteratively updated using gradient descent. This yields a thrust allocation that best approximates the

intended direction while accounting for the actual motor thrust directions.

Finally, the obtained thrust coefficients α are multiplied by a gain to compute the thrust value for each motor, which is then converted into PWM values for real-world control. The PWM values are calculated using a PWM-thrust approximation model derived from motor unit tests. To prevent excessive thrust output, the PWM values are limited to a maximum of 0.7. This ensures that the haptic feedback presented to the user remains within a safe and stable range.

C. Mode Switching Strategy for Haptic Presentation

The robot switches between two types of haptic feedback to adapt the interaction to the user's situation.

- **Vibration feedback**
  The outputs of two motors on each side of the user's arm are alternated to generate a periodic vibration pattern. This vibration serves as a signal to restart guidance when the arm is lowered and the user moves away from the target, and it is also used to indicate arrival at the target.
- **Pulse Direction feedback**
  The haptic direction computed in Section II-B is presented intermittently as a pulse sequence. Compared with continuous output, pulsed feedback makes the presented direction easier to perceive. Furthermore, the number of pulses varies with the distance to the target, allowing the user to intuitively sense how far to move.

According to the user's situation, these haptics feedback are switched following the flowchart shown in Fig. 4 based on three factors as followed:

1) **Relative distance to the target**
   The distance is defined as

$$\delta = \|\mathbf{v}_{target}\| \tag{6}$$

   The user is classified as "arrived" if $\delta < \theta_{close}$, as "medium distance" if $\theta_{mid} \leq \delta < \theta_{far}$, and as "far" if $\delta \geq \theta_{far}$.
2) **User's arm posture**
   The user's arm posture (raised or lowered) is classified from the roll angle ϕ and pitch angle θ obtained from the robot's attitude during perching as follows:

$$s_{arm} = \begin{cases} 1 & (|\phi| < \theta_{\text{roll}},\ |\theta| < \theta_{\text{pitch}}) \\ 0 & \text{otherwise} \end{cases} \tag{7}$$

   where $s_{arm} = 1$ indicates that the arm is raised, and $s_{arm} = 0$ indicates that it is lowered.
3) **Directional alignment with target**
   Whether the user is moving in the target direction is evaluated by the inner product. Using the last robot position $\mathbf{p}_{last}$, the displacement vector is defined as

$$\Delta\mathbf{p} = \mathbf{p}_{current} - \mathbf{p}_{last} \tag{8}$$

   and the alignment is computed as

$$d = \frac{\mathbf{v}_{target}}{\|\mathbf{v}_{target}\|} \cdot \frac{\Delta\mathbf{p}}{\|\Delta\mathbf{p}\|} \tag{9}$$

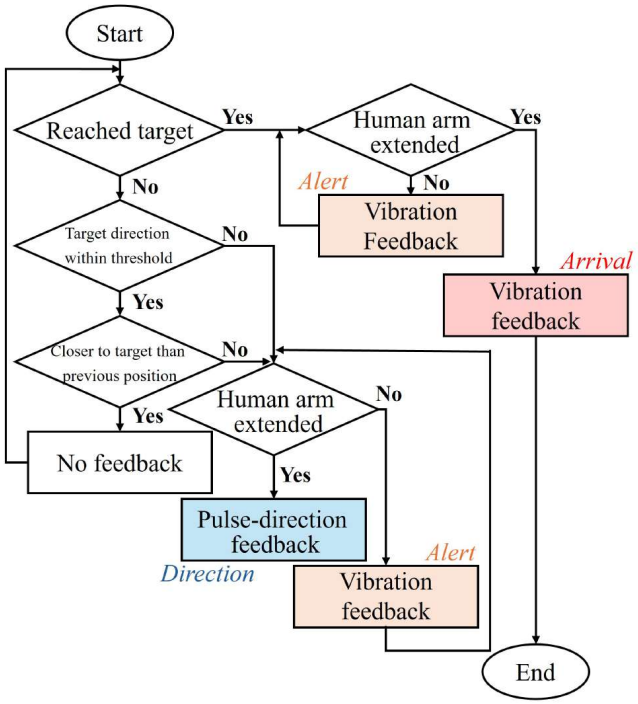

Fig. 4. Flowchart of mode switching for haptic feedback

If $d > \theta_{dir}$, the movement is considered aligned with the target direction. Otherwise, it is considered deviated.

Combining these conditions, the haptics mode m is defined as:

$$m = \begin{cases} \textit{Arrival} & \delta \leq \theta_{close} \\ \textit{Alert} & (d \leq \theta_{dir}) \ \vee \ (s_{arm} = 0) \\ \textit{Direction} & (d > \theta_{dir}) \ \wedge \ (s_{arm} = 1) \ \wedge \ (\delta > \theta_{close}) \end{cases} \tag{10}$$

Based on this haptics mode, as illustrated in Fig. 4, the feedback is switched following the user's situation. Immediately after perching, pulse feedback is always initiated to begin guidance. In *Alert mode*, vibration feedback serves as a signal to restart guidance when the arm is lowered and the user moves away from the target. Once the arm is raised again, the system resumes pulse feedback to indicate the correct direction in *Direction mode*. In *Direction mode*, the number of pulses is determined by the distance:

$$N_{pulse} = \begin{cases} 1 & (\delta < \theta_{mid}) \\ 2 & (\theta_{mid} \leq \delta < \theta_{far}) \\ 3 & (\delta \geq \theta_{far}) \end{cases} \tag{11}$$

This allows the user to intuitively perceive both direction and distance.

When the user is sufficiently close to the target ($\delta \leq \theta_{close}$), *Arrival mode* is triggered, and a short vibration notifies task completion before all motors are stopped. Unlike the vibration used in *Alert mode* during guidance, this arrival signal is presented when the arm is raised.

If none of the conditions apply and the user is already moving correctly toward the target, feedback is suppressed.

This ensures energy efficiency and allows natural walking to continue without interference.

As a result, by integrating position, posture, and movement information to switch between modes, the proposed method achieves intuitive and context-aware haptic guidance. In addition to conveying direction and distance, vibrations highlight key events such as errors and arrival, providing guidance that is both diverse and easy to interpret.

III. Experiment

A. Measurement of Haptic Force and Direction Characteristics

In this experiment, we measured the presented haptic force characteristics generated during perching when each motor was activated. An arm model was placed above the sensing surface of a force sensor, and the aerial robot was perched on top so that the generated forces were transmitted directly to the sensor. The four motors are arranged diagonally in the xy-plane of the body coordinate system, each positioned at 90° intervals. Specifically, Motor 0 is oriented along ($\cos 135°$, $\sin 135°$), Motor 1 along ($\cos 45°$, $\sin 45°$), Motor 2 along ($\cos -45°$, $\sin -45°$), and Motor 3 along ($\cos -135°$, $\sin -135°$). The inflatable actuators in the arm joints were pressurized to 50 kPa and those at the contact surfaces to 20 kPa, with both pressures maintained constant throughout the experiment. Under the driving conditions, the PWM input to each motor was increased in 0.25 increments. Each motor was driven for 5 s, followed by 1 s at PWM 0.5 to stop, and this cycle was repeated. The magnitude of the presented haptic force was calculated by combining the x- and y-axis components measured by the force sensor and averaging the values after low-pass filtering. The force direction (in degrees) was computed from the x and y components and averaged over PWM inputs ranging from 0.65 and 0.8.

The results, organized at every 0.5 step of PWM input, are summarized in Table I. From the results in Table I, the presented haptic force generally increased monotonically with PWM values, reaching a maximum of approximately 2.61 N under single-motor actuation. However, variations were observed across motors, with motor 0 producing noticeably smaller outputs than the others. For dual-motor actuation, the presented force was evaluated as the vector sum of the individually measured single-motor outputs, assuming an ideal motor configuration. Combinations such as motor 1&2, motor 0&1, and motor 3&0 showed close agreement between predicted and experimental results in both magnitude and direction (e.g., for 1&2 at PWM 0.8, the predicted value was 3.33 N and the measured value was 3.31 N). In contrast, motor 2&3 produced 3.53 N compared to the predicted 2.52 N, indicating a larger magnitude.

Regarding output direction, single-motor actuation showed that motors 1, 2, and 3 matched the ideal angles (±45°, ±135°) within ±2°, whereas motor 0 exhibited a deviation of about ±10°. For dual-motor actuation, the output directions generally aligned with the theoretical vector sums, however, deviations of about ±10–20° were observed.

TABLE I
Measured force at each PWM value and direction

Motor Number	Force at each PWM value(N)						Degree
	0.55	0.6	0.65	0.7	0.75	0.8	
0	0.14	0.29	0.55	0.74	0.89	1.06	145.15
1	0.17	0.42	0.92	1.37	1.98	2.33	42.79
2	0.13	0.43	0.91	1.34	1.98	2.38	-43.52
3	0.27	0.52	0.42	0.99	2.01	2.61	-134.94
0&1	0.19	0.63	1.25	1.66	2.11	2.31	69.63
1&2	0.24	0.61	1.19	2.15	3.02	3.31	16.11
2&3	0.23	0.60	0.77	1.20	1.96	2.52	-79.15
3&0	0.29	0.51	1.03	1.26	2.23	2.91	-160.43

These discrepancies of presented haptic force and direction are attributed to motor and structural variations, as well as differences in the deforming posture of the arm during perching, which caused part of the force to escape in the vertical direction and reduced the horizontal component.

Nevertheless, when considering haptic forces to humans, both force magnitude and directional accuracy must remain within perceptual thresholds to ensure effective and safe interaction. Previous studies have reported that humans can perceive forces greater than 0.04 N [47] and discriminate angular deviations up to approximately 25° [48]. In this study, even at PWM 0.55, more than 0.1 N was produced, confirming that the generated forces were sufficiently above the perceptual threshold. Furthermore, deviations in output direction remained within the reported perceptual threshold of 25°, demonstrating that the presented cues were both reliably recognizable and practically valid for haptic guidance.

At the same time, single-motor actuation yielded an average output exceeding 1.0 N, so the maximum PWM input was limited to 0.7 in this study in order to avoid excessive forces and ensure user safety. Under this condition, the average power consumption during flight was approximately 288.7 W, whereas driving a single motor at the upper limit of PWM 0.7 required only about 80.7 W, and even with two motors operating simultaneously, the consumption was at most 161.4 W, corresponding to about 56% of the flight power. Furthermore, in actual haptic guidance, two motors were typically driven up to around PWM 0.65, where the average power consumption remained about 95.0 W, equivalent to only 33% of the flight condition. Thus, haptic guidance in the proposed method requires only about half the power of flight at the maximum setting, and is considered to consume significantly less energy than flight-based approaches.

B. Experimental Validation of Haptic Guidance Method

To evaluate the effectiveness of the proposed haptic guidance method, we conducted an experiment in which participants were guided to a target position as shown in Fig. 5A. The aerial robot used in this study has a total mass of 1.444 kg and overall dimensions of $350 \times 350 \times 250$ mm. All experiments were conducted in a controlled indoor environment under supervision. The maximum available thrust is approximately 8 N per rotor, providing sufficient thrust margin for stable flight and perching.

Participants wore eye masks to block vision and headphones to block hearing. The target location was not disclosed in advance, and participants were instructed to rely

solely on the haptic cues provided by the robot.

The robot's current position was tracked using a motion capture system, and the target position was set at $(x, y) = (3.0\,\mathrm{m}, -1.0\,\mathrm{m})$ relative to the starting position. The experiment began with the robot perching on the participant's arm. Using the method described in Section II-B, the robot provided pulsed haptic cues to indicate the direction of movement, and upon arrival at the goal, a short vibration was presented as an arrival signal.

The results are shown in Fig. 5B and C. As denoted in Fig. 5B, the participant's trajectory exhibited a cyclic increase-decrease pattern. This suggests that participants repeatedly corrected their path based on the pulsed directional cues. In some instances, as denoted in Fig. 5C, the time history of the tracking error revealed deviations of up to approximately 1.25 m, but the error was reduced to around 0.2 m, confirming that the guidance information was effectively utilized.

In addition, as shown in Fig. 5B, a comparison between the measured trajectories and the ideal straight-line path further showed that, although participants moved with some meandering, they remained close to the ideal line and successfully reached the target. The pulsed cues effectively supported incremental corrections, while the short vibration at arrival was consistently recognized as a completion signal.

These results demonstrate that the proposed method can guide users to a target position relying solely on haptic feedback, even when vision and hearing are blocked. On the other hand, temporary deviations of up to 1.25 m were observed, resulting in zigzag trajectories. Such deviations are likely due to factors such as cue timing, intensity, or response delays, suggesting that optimizing the feedback parameters could further improve guidance accuracy.

C. Perching and Haptics Sequence Experiment

To verify the effectiveness of the integrated perching-based haptic guidance process, we conducted a series of scenario experiments with human participants. The robot's position was tracked using a motion capture system, and the target location was randomly set within $-0.8\,\mathrm{m} < x < -1.5\,\mathrm{m}$ and $-0.5\,\mathrm{m} < y < -1.2\,\mathrm{m}$ without informing the participants. In this experiment, the target was set at $(x, y) = (1.4\,\mathrm{m}, -0.95\,\mathrm{m})$ relative to the starting position.

As illustrated in Fig. 6A, the experimental procedure is conducted as follows:

1) **Approach Phase:** The robot detected the participant using its onboard camera and approached.
2) **Perch Phase:** The robot landed on and grasped the forearm. Pneumatic actuation deformed the arm to adapt to the forearm.
3) **Haptic Guidance Phase:** While perched, thrust distribution provided haptic guidance toward the target.
4) **Deperch Phase:** After arrival, the robot took off (deperch).

In the perch phase, the robot descended approximately 0.16 m and landed on the participant's forearm by inflating the joint actuators as shown in Fig. 6A(4) and D. Immediately after contact, the pressures were 12 kPa at the joints

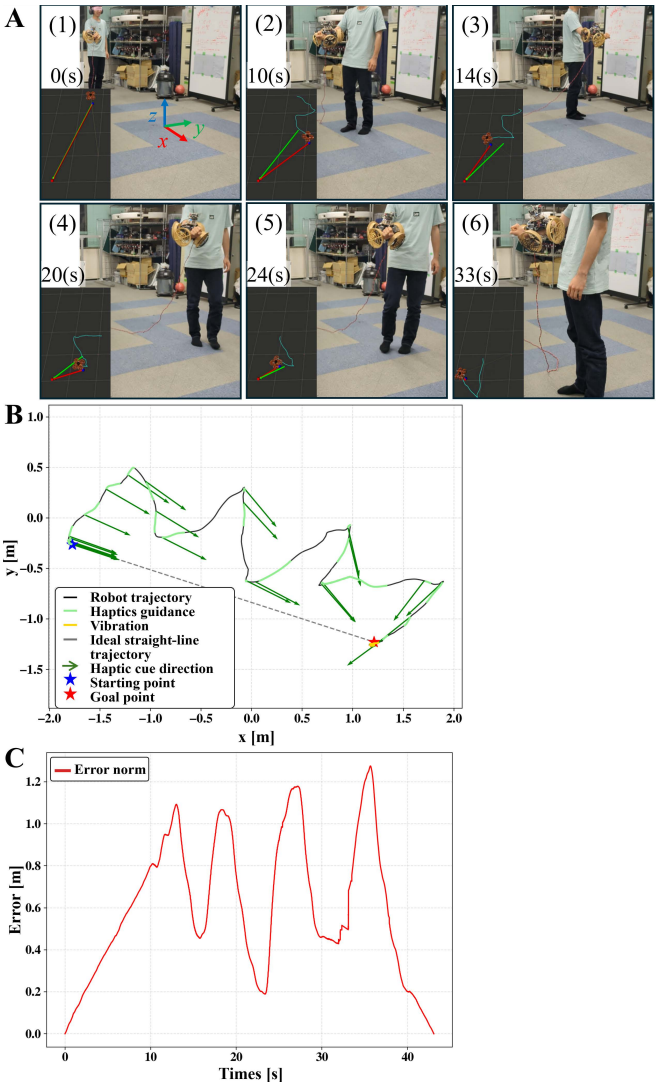

Fig. 5. Overview of the perching-based haptic guidance experiment. (A) Scenario snapshots of the haptic guidance experiment. (B) Participant trajectory with haptic guidance. (C) Tracking error over time.

and 20 kPa at the contact surfaces. These values equalized to about 19 kPa within 0.3 s and reached the target pressure within 3.5 s, indicating rapid stabilization following landing.

In the haptic guidance phase, Fig. 6A(6) shows that pulsed cues enabled the participant to recognize and follow the intended direction. Fig. 6A(7) illustrates that when the participant lowered their arm, vibration feedback prompted corrective motion and a brief vibration signaled task completion upon reaching the target as shown in Fig. 6A(8). Additionally, Fig. 6D indicates that during haptic guidance, the pressures remained stable at approximately 50 kPa at the joints and 21 kPa at the contact surfaces, ensuring secure grasping even when the participant's arm posture changed.

As shown in Fig. 6B, the presented haptic force vectors were generally aligned with the participant's trajectory, indicating that the cues effectively supported directional correction. The trajectory analysis in Fig. 6C reveals that although deviations of up to 0.6 m occurred, the participant reached the target within approximately 20 s, demonstrating the feasibility of haptic-based guidance. Overall, the results

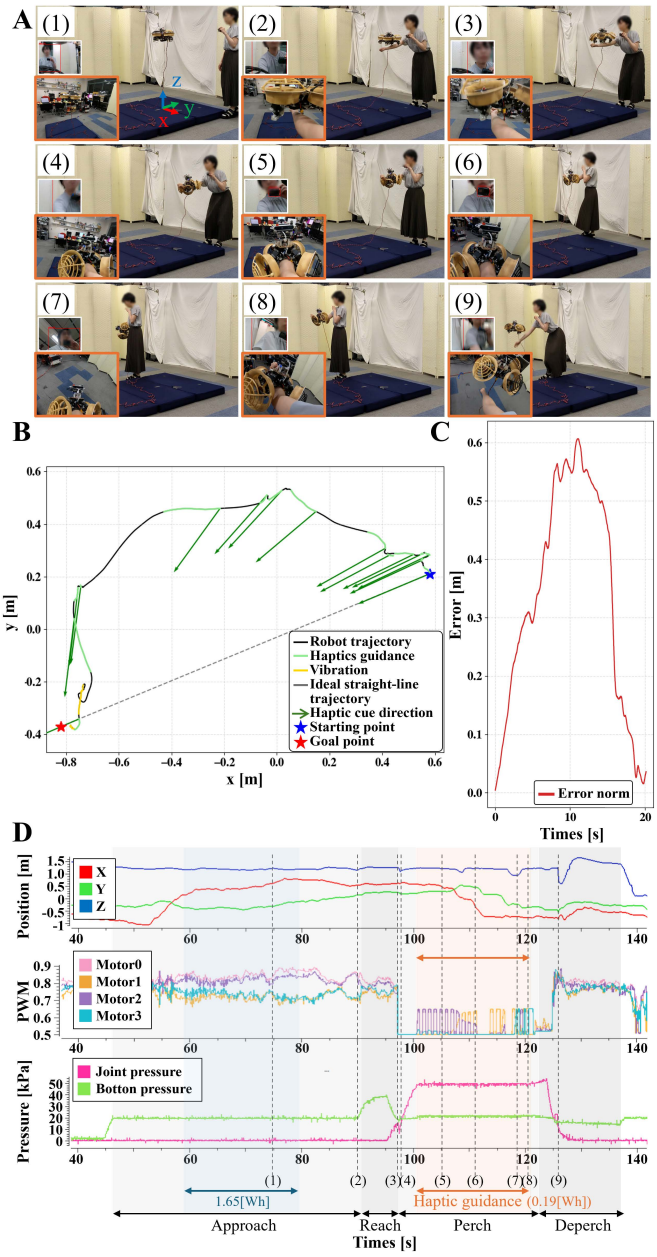

Fig. 6. Scenario experiment of perching-based haptic guidance. (A) Snapshots showing the experimental sequence of approach, perching, haptic guidance, and deperching. (B) Participant trajectory with overlaid haptic cue directions compared to the ideal straight-line path. (C) Time history of trajectory error norm. (D) The data including position, motor PWM commands, and pneumatic pressures throughout the experiment.

indicate that both pulsed cues for directional guidance and vibration signals for arrival were effective, enabling intuitive and reliable navigation assistance.

Energy consumption during flight and perching-based haptic guidance was estimated from battery voltage logs and a PWMcurrent calibration table over a matched 20 s interval, with sparse PWM data reconstructed using zero-order hold method. During flight, the estimated total energy consumption was 1.65 Wh (297.4 W average power), whereas perching-based haptic guidance consumed 0.19 Wh (35.3 W average power). This corresponds to an 88.1% reduction in energy use under the perching condition. These results indicate that, once physical contact is established, haptic guidance via perching can be achieved with substantially lower energy demand than sustained flight.

Finally, the deperch phase was completed safely, and the entire process was carried out without any discomfort or risk to the participant. These results confirm that the system can stably achieve the entire support process, Approach, Perch, Haptic Guidance, and Deperch, establishing a new framework for pHDI based on close physical contact.

IV. Conclusion

In this study, we proposed a perching-based haptic guidance method in which an aerial robot perches directly on the human arm and provides guidance through thrust-based cues and vibration feedback, while ensuring safe and adaptive contact. Furthermore, we implemented context-dependent switching between two types of haptic feedback to adapt the interaction to the user's situation.

User experiments demonstrated that participants could reliably reach target positions without significant deviation under vision- and hearing-blocked conditions, while the presented forces and directions remained within human perceptual thresholds. Moreover, the robot consistently executed the entire sequence of approach, perching, haptic guidance, and deperch, validating the feasibility of proposed method. These results extend conventional non-contact or constrained HDI approaches, establishing a new framework of close pHDI that offers intuitive, stable, and energy-efficient support.

In future work, we will improve the haptic guidance control method by reflecting the result presented in Section III-A and Section III-B, as well as insights from additional user studies on human perception. We also plan to extend the system to handle more complex trajectories and diverse environments, enabling robust navigation beyond simple paths. In addition, we will explore landing strategies to human arm that combine pneumatic actuation with thrust control, allowing adaptive arm deformation for more precise and versatile perching. Overall, these efforts will advance the system toward more natural and versatile pHDI.

References

[1] M. A. Goodrich, A. C. Schultz, *et al.*, "Human–robot interaction: a survey," *Foundations and trends® in human–computer interaction*, vol. 1, no. 3, pp. 203–275, 2008.

[2] R. R. Murphy, "Human-robot interaction in rescue robotics," *IEEE Transactions on Systems, Man, and Cybernetics, Part C (Applications and Reviews)*, vol. 34, no. 2, pp. 138–153, 2004.

[3] V. Herdel, L. J. Yamin, and J. R. Cauchard, "Above and beyond: A scoping review of domains and applications for human-drone interaction," in *Proc. CHI Conf. on Hum. Factors Comput. Syst.*, 2022, pp. 1–22.

[4] S. N. Lingam, M. Franssen, S. M. Petermeijer, and M. Martens, "Challenges and future directions for human-drone interaction research: an expert perspective," *International Journal of Human–Computer Interaction*, vol. 41, no. 12, pp. 7905–7921, 2025.

[5] D. Tezza and M. Andujar, "The state-of-the-art of humandrone interaction: A survey," *IEEE Access*, vol. 7, pp. 167 438–167 454, 2019.

[6] M. Avila, M. Funk, and N. Henze, "Dronenavigator: Using drones for navigating visually impaired persons," in *Proc. 17th International ACM SIGACCESS Conf. on Computers & Accessibility*, 2015, pp. 327–328.

[7] M. Avila Soto, M. Funk, M. Hoppe, R. Boldt, K. Wolf, and N. Henze, "Dronenavigator: Using leashed and free-floating quadcopters to navigate visually impaired travelers," in *Proc. 19th international acm sigaccess Conf. on computers and accessibility*, 2017, pp. 300–304.

[8] A. Colley, L. Virtanen, P. Knierim, and J. Häkkilä, "Investigating drone motion as pedestrian guidance," in *Proc. 16th Int. Conf. Mobile and Ubiquitous Multimedia*, 2017, pp. 143–150.

[9] M. Tognon, R. Alami, and B. Siciliano, "Physical human-robot interaction with a tethered aerial vehicle: Application to a force-based human guiding problem," *IEEE Transactions on Robotics*, vol. 37, no. 3, pp. 723–734, 2021.

[10] F. Huppert, G. Hoelzl, and M. Kranz, "Guidecopter-a precise drone-based haptic guidance interface for blind or visually impaired people," in *Proc. CHI Conf. on Hum. Factors Comput. Syst.*, 2021, pp. 1–14.

[11] D. Floreano and R. J. Wood, "Science, technology and the future of small autonomous drones," *Nature*, vol. 521, pp. 460–466, 2015.

[12] V. Kumar and N. Michael, "Opportunities and challenges with autonomous micro aerial vehicles," *The International Journal of Robotics Research*, vol. 31, no. 11, pp. 1279–1291, 2012.

[13] R. Bonatti, Y. Zhang, S. Choudhury, W. Wang, and S. Scherer, "Autonomous drone cinematographer: Using artistic principles to create smooth, safe, occlusion-free trajectories for aerial filming," in *Proc. of the 2018 international symposium on experimental robotics*. Springer, 2020, pp. 119–129.

[14] F. Chataigner, "Arsi: an aerial robot for sewer inspection." *Advances in Robotics Research: From Lab to Market. Springer, Cham, 2020*, pp. 249–274, 2020.

[15] N. Michael, S. Shen, K. Mohta, Y. Mulgaonkar, V. Kumar, K. Nagatani, Y. Okada, S. Kiribayashi, K. Otake, K. Yoshida, K. Ohno, E. Takeuchi, and S. Tadokoro, "Collaborative mapping of an earthquake-damaged building via ground and aerial robots," *Journal of Field Robotics*, vol. 29, no. 5, pp. 832–841, 2012.

[16] T. W. Danko, A. Kellas, and P. Y. Oh, "Robotic rotorcraft and perch-and-stare: Sensing landing zones and handling obscurants," in *Proc. ICAR'05. Proceedings., 12th Int. Conf. Advanced Robotics, 2005.* IEEE, 2005, pp. 296–302.

[17] A. McLaren, Z. Fitzgerald, G. Gao, and M. Liarokapis, "A passive closing, tendon driven, adaptive robot hand for ultra-fast, aerial grasping and perching," in *Proc. IEEE/RSJ Int. Conf. Intell. Robots Syst. (IROS)*. IEEE, 2019, pp. 5602–5607.

[18] P. E. I. Pounds, D. R. Bersak, and A. M. Dollar, "Grasping from the air: Hovering capture and load stability," in *Proc. IEEE Int. Conf. Robot. Autom.*, 2011, pp. 2491–2498.

[19] S. Lin, A. Lynch, and M. Liarokapis, "An ultra-light, ultra-fast, passive closing aerial gripping system capable of grasping, perching, and aerial manipulation," in *Proc. IEEE Int. Symp. on Safety, Security, Rescue Robot. (SSRR)*. IEEE, 2024, pp. 12–17.

[20] H. Zhang, J. Sun, and J. Zhao, "Compliant bistable gripper for aerial perching and grasping," in *Proc. Int. Conf. Robot. Autom. (ICRA)*, 2019, pp. 1248–1253.

[21] Y. Zhao, R. Xiang, H. Li, C. Wang, J. Zhang, X. Liu, and Y. Hao, "Design and validation of a biomimetic leg-claw mechanism capable of perching and grasping for multirotor drones," *Biomimetics*, vol. 10, no. 1, p. 10, 2024.

[22] W. R. Roderick, M. R. Cutkosky, and D. Lentink, "Bird-inspired dynamic grasping and perching in arboreal environments," *Science Robotics*, vol. 6, no. 61, p. eabj7562, 2021.

[23] S. Ubellacker, A. Ray, J. M. Bern, J. Strader, and L. Carlone, "High-speed aerial grasping using a soft drone with onboard perception," *npj Robotics*, vol. 2, no. 1, p. 5, 2024.

[24] C. E. Doyle, J. J. Bird, T. A. Isom, J. C. Kallman, D. F. Bareiss, D. J. Dunlop, R. J. King, J. J. Abbott, and M. A. Minor, "An avian-inspired passive mechanism for quadrotor perching," *IEEE/ASME Transactions On Mechatronics*, vol. 18, no. 2, pp. 506–517, 2012.

[25] P. H. Nguyen, K. Patnaik, S. Mishra, P. Polygerinos, and W. Zhang, "A soft-bodied aerial robot for collision resilience and contact-reactive perching," *Soft Robotics*, 2023.

[26] D. Sarkar, A. Arora, S. Sen, S. S. S. Katta, D. Shashank, M. Rohan, and S. K. Saha, "Development of an autonomous uav integrated with a manipulator and a soft gripper," in *Proc. 13th Asian Control Conf. (ASCC)*, 2022, pp. 2212–2217.

[27] J. T. Ping, B. H. Khoo, O. A. Syadiqeen, N. Khoo, C. P. Tan, and S. G. Nurzaman, "Aerial grasping by a quadrotor uav with a soft material gripper."

[28] H. C. Cheung, C.-W. Chang, B. Jiang, C.-Y. Wen, and H. K. Chu, "A modular pneumatic soft gripper design for aerial grasping and landing," in *Proc. IEEE 7th Int. Conf. Soft Robot. (RoboSoft)*, 2024, pp. 82–88.

[29] W. Tao, K. Patnaik, F. Chen, Y. Kumar, and W. Zhang, "Design, characterization and control of a whole-body grasping and perching (whopper) drone," in *Proceedings of the 2018 international symposium on experimental robotics*. IEEE, 2023, pp. 1–7.

[30] F. Ruiz, B. C. Arrue, and A. Ollero, "Sophie: Soft and flexible aerial vehicle for physical interaction with the environment," *IEEE Robotics and Automation Letters*, vol. 7, no. 4, pp. 11 086–11 093, 2022.

[31] P. Zheng, F. Xiao, P. H. Nguyen, A. Farinha, and M. Kovac, "Metamorphic aerial robot capable of mid-air shape morphing for rapid perching," *Scientific Reports*, vol. 13, no. 1, p. 1297, 2023.

[32] N. Bucki, J. Tang, and M. W. Mueller, "Design and control of a midair-reconfigurable quadcopter using unactuated hinges," *IEEE Transactions on Robotics*, vol. 39, no. 1, pp. 539–557, 2022.

[33] A. Miyamichi, M. Zhao, K. Sugihara, J. Sugihara, M. Konishi, K. Kojima, K. Okada, and M. Inaba, "Flexible morphing aerial robot with inflatable structure for perching-based human-robot interaction," 2025. [Online]. Available: https://arxiv.org/abs/2509.07496

[34] J. R. Cauchard, A. Tamkin, C. Y. Wang, L. Vink, M. Park, T. Fang, and J. A. Landay, "Drone.io: A gestural and visual interface for human-drone interaction," in *Proc. 14th ACM/IEEE Int. Conf. Human-Robot Interaction (HRI)*, 2019, pp. 153–162.

[35] M. Obaid, F. Kistler, G. Kasparavičiūtė, A. E. Yantaç, and M. Fjeld, "How would you gesture navigate a drone? a user-centered approach to control a drone," in *Proc. 20th International Academic Mindtrek Conf.*, 2016, pp. 113–121.

[36] J. R. Cauchard, K. Y. Zhai, M. Spadafora, and J. A. Landay, "Emotion encoding in human-drone interaction," in *Proc. 11th ACM/IEEE Int. Conf. Human-Robot Interaction (HRI)*. IEEE, 2016, pp. 263–270.

[37] V. Herdel and J. R. Cauchard, "Emotion appropriateness in human–drone interaction," *International Journal of Social Robotics*, vol. 16, no. 3, pp. 579–597, 2024.

[38] V. Herdel, A. Kuzminykh, A. Hildebrandt, and J. R. Cauchard, "Drone in love: Emotional perception of facial expressions on flying robots," in *Proc. CHI Conf. on Hum. Factors Comput. Syst.*, 2021, pp. 1–20.

[39] M. Seuter, E. R. Macrillante, G. Bauer, and C. Kray, "Running with drones: desired services and control gestures," in *Proc. 30th Australian Conf. on Computer-Human Interaction*, 2018, pp. 384–395.

[40] F. Mueller and M. Muirhead, "Jogging with a quadcopter," in *Proc. 33rd Annual ACM Conf. on Hum. Factors Comput. Syst.*, 2015, pp. 2023–2032.

[41] S. G. Zwaan and E. I. Barakova, "Boxing against drones: Drones in sports education," in *Proc. The 15th Int. Conf. Interaction Design and Children*, 2016, pp. 607–612.

[42] S. Sanz-Martos, M. D. Lpez-Franco, C. lvarez Garca, N. Granero-Moya, J. M. Lpez-Hens, S. Cmara-Anguita, P. L. Pancorbo-Hidalgo, and I. M. Comino-Sanz, "Drone applications for emergency and urgent care: A systematic review," *Prehospital and Disaster Medicine*, vol. 37, no. 4, pp. 502–508, 2022.

[43] T. Jain, A. Sibley, H. Stryhn, and I. Hubloue, "Comparison of unmanned aerial vehicle technology-assisted triage versus standard practice in triaging casualties by paramedic students in a mass-casualty incident scenario," *Prehospital and Disaster Medicine*, vol. 33, no. 4, pp. 375–380, 2018.

[44] S. M. S. M. Daud, M. Y. P. M. Yusof, C. C. Heo, L. S. Khoo, M. K. C. Singh, M. S. Mahmood, and H. Nawawi, "Applications of drone in disaster management: A scoping review," *Science and Justice*, vol. 62, no. 1, pp. 30–42, 2022.

[45] P. Anderson, "A bird in the house: An anthropological perspective on companion parrots," *Society & Animals*, vol. 11, no. 4, pp. 393–418, 2003.

[46] P. K. Anderson, "Social dimensions of the human–avian bond: parrots and their persons," *Anthrozoös*, vol. 27, no. 3, pp. 371–387, 2014.

[47] S. Feyzabadi, S. Straube, M. Folgheraiter, E. A. Kirchner, S. K. Kim, and J. C. Albiez, "Human force discrimination during active arm motion for force feedback design," *IEEE transactions on haptics*, vol. 6, no. 3, pp. 309–319, 2013.

[48] J. Hong, L. Stearns, J. Froehlich, D. Ross, and L. Findlater, "Evaluating angular accuracy of wrist-based haptic directional guidance for hand movement." in *Proc. Graphics Interface*, 2016, pp. 195–200.